Software Based Technique for the Identification of Transformer Faults in Real Time

By

A. Abu-Siada

SECOND PAGE IS LEFT BLANK

Soft Ware Based Technique for the Identification of Transformer Faults in Real Time

A. Abu-Siada

Curtin University

Abstract

Frequency Response Analysis (FRA) has been growing in popularity in recent times as a tool to detect mechanical deformation within power transformers. To conduct the test, the transformer has to be taken out of service which may cause interruption to the electricity grid. Moreover, because FRA relies on graphical analysis, it calls for an expert person to analyse the results as so far, there is no standard code for FRA interpretation worldwide. In this paper an online technique is introduced to detect the internal faults within a power transformer by considering the voltage-current (*V-I*) locus diagram as a transformer fingerprint that can be measured every cycle to provide a current state of the transformer. The technique does not call for any special equipment as it uses the existing metering devices attached to any power transformer to monitor the input voltage, output voltage and the input current at the power frequency and hence online monitoring can be realised. Various types of faults have been simulated to assess its impact on the proposed locus. A Matlab code based on digital image processing is developed to calculate any deviation of the *V-I* locus with respect to the reference one and to identify the type of fault. The proposed technique is easy to implement and automated so that the requirement for expert personnel can be eliminated.

Introduction

Power transformers are critical links within any transmission or distribution network. In service transformer faults are not only causing extended outages, but costly repairs and potentially serious injury or fatality can result. The majority of transformers currently in service worldwide were installed prior to 1980 and as a result the bulk of the population is approaching or has already exceeded its design life which increases the likelihood of transformer failure [1]. This poses a significant risk for utilities and other power network stakeholders as the impact of an in service transformer failure can be catastrophic. The mechanical forces that a transformer is exposed to during faults, switching transients and other system events result in magnetic forces being imposed on the windings. If these forces exceed the withstand capability of the transformer, winding deformation may occur. Loss of clamping pressure due to insulation degradation caused by ageing can also lead to mechanical damage to transformer windings. While with only minor winding damage the transformer is still capable of normal operation, its ability to withstand faults is greatly reduced which makes it essential to detect even slight winding deformation as early as possible. Transformers are expected to survive a number of short circuit faults without failure but once any significant winding deformation is produced, the likelihood of surviving further short circuits is greatly reduced because of the locally increased electromagnetic stresses. Furthermore, any reduction in winding clamping due to insulation shrinkage caused by ageing will also increase the probability of failure by reducing the mechanical strength of the winding assemblies [2]. Winding deformation can take many forms including radial buckling, conductor tilting, spiral tightening and collapse of the winding end supports which are difficult to detect using traditional testing techniques [3]. Frequency response analysis (FRA) is a powerful diagnostic method in detecting winding deformation and clamping structure for power transformers [4]. Since transformer windings can be modelled as a network of distributed capacitors, resistors, self and mutual inductors; values of these parameters are altered upon fault occurrence within the winding which accordingly affects the

winding frequency response. The FRA test is conducted by applying a sweep frequency voltage of low amplitude to a transformer terminal and measuring the response voltage across the other terminal of the same winding with reference to the tank [5]. While the testing method is relatively simple since the development of specific FRA test equipment, the interpretation of results remains a highly specialised area and requires expert personnel to determine the type and possible location of the fault [6]. The main drawback of FRA test is that the transformer has to be switched off and taken out of service which may cause interruption to the power network. To prevent network interruption due to transformer outage for testing and to reduce the need for specialist to conduct the FRA test and to interpret its results, an alternative on-line technique to detect internal mechanical faults inside the transformer is required. This paper introduces a new on line technique that is relying on constructing a locus between the voltage difference in the high and the low voltage sides of a particular phase against its input current. A digital image processing technique is developed to compare the healthy and faulty loci to identify the type of fault. Unlike FRA which uses a sweep frequency in the range of 2 MHz, this technique is performed at the power frequency and hence online monitoring of transformer mechanical condition can be realised. Moreover, the method does not call for any additional equipment as it uses the metering equipment attached to any power transformer to monitor the input/output voltages and the input current. Also, the method does not call for an expert person to conduct or to analyse the results.

Proposed technique

The proposed technique depends on constructing a locus diagram relating the transformer input current on the x-axis and the difference between the input and output voltages of a particular phase on the y-axis. The relationship relating the above parameters can be derived using the single phase transformer equivalent circuit and its phasor diagram shown in Fig. 1.
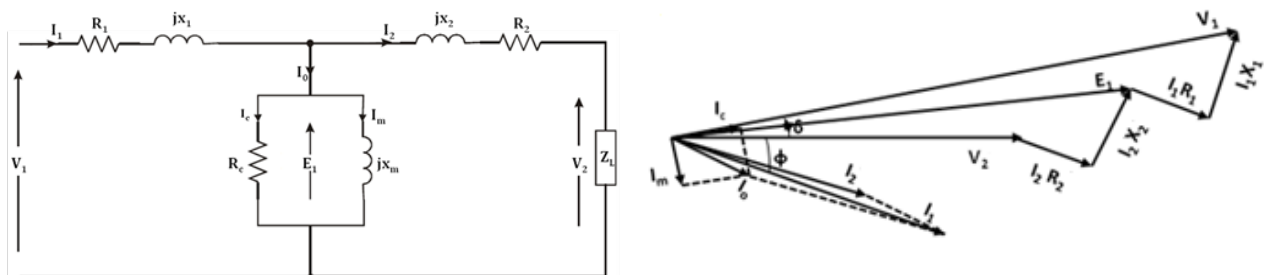

Figure 1
Per-unit equivalent circuit of transformer and Phasor diagram

Let:

$$v_2(t) = V_{m2}\sin(\omega t) \tag{1}$$

$$v_1(t) = V_{m1}\sin(\omega t + \delta) \tag{2}$$

$$x = i_1(t) = I_{m1}\sin(\omega t - \varphi) \tag{3}$$

For simplicity, assume $V_{m1} = V_{m2} = V_m$

$$y = v_1 - v_2 = V_m\{\sin(\omega t + \delta) - \sin(\omega t)\} \tag{4}$$

$$\Rightarrow y = 2V_m\cos(\omega t + \frac{\delta}{2}) \cdot \cos(\delta) \tag{5}$$

Cartesian formula relating *x* and *y* can be obtained from the parametric equations (3) and (5) by

eliminating *wt*.

From (3) and (5):

$$\omega t = \sin^{-1}(\frac{x}{I_{m1}}) + \varphi = \cos^{-1}(\frac{y}{2V_m \cos \delta}) - \frac{\delta}{2} \Rightarrow \left\{ \cos^{-1}\frac{y}{2V_m \cos \delta} - \sin^{-1}\frac{x}{I_{m1}} \right\} = (\varphi + \frac{\delta}{2})$$

$$\Rightarrow \sin\left\{ \cos^{-1}\frac{y}{2V_m \cos \delta} - \sin^{-1}\frac{x}{I_{m1}} \right\} = \sin(\varphi + \frac{\delta}{2})$$

$$\Rightarrow \sin(\cos^{-1}\frac{y}{2V_m \cos \delta}) \cdot \cos(\sin^{-1}\frac{x}{I_{m1}}) - \cos(\cos^{-1}\frac{y}{2V_m \cos \delta}) \cdot \sin(\sin^{-1}\frac{x}{I_{m1}}) = \sin(\varphi + \frac{\delta}{2})$$

$$\Rightarrow \frac{\sqrt{(2V_m \cos \delta)^2 - y^2}}{2V_m \cos \delta} \cdot \frac{\sqrt{I_m^2 - x^2}}{I_{m1}} - \frac{y}{2V_m \cos \delta} \cdot \frac{x}{I_{m1}} = \sin(\varphi + \frac{\delta}{2})$$

$$\Rightarrow \sqrt{\{(2V_m \cos \delta)^2 - y^2\} \cdot \{I_{m1}^2 - x^2\}} = 2V_m I_{m1} \cos \delta \sin(\varphi + \frac{\delta}{2}) + xy \qquad (6)$$

Squaring both sides and rearranging the equation:

$$(2V_m \cos \delta)^2 x^2 + 4V_m I_{m1} \cos \delta \sin(\varphi + \frac{\delta}{2})xy + I_{m1}^2 y^2 + (2V_m I_{m1} \cos \delta \sin(\varphi + \frac{\delta}{2}))^2 - (2V_m I_{m1}\cos\delta)^2 = 0 \quad (7)$$

Assume the coefficients of (7) are:

$$A = (2V_m \cos \delta)^2; \; B = 4V_m I_{m1} \cos \delta \sin(\varphi + \frac{\delta}{2}); C = I_{m1}^2; D = (2V_m I_{m1} \cos \delta \sin(\varphi + \frac{\delta}{2}))^2 - (2V_m I_{m1}\cos\delta)^2$$

The quadratic equation (7) represents [7]

An ellipse if $B^2 - 4AC \prec 0$; a parabola if $B^2 - 4AC = 0$; a hyperbola if $B^2 - 4AC \succ 0$

$$B^2 - 4AC = 16I_{m1}^2 V_m^2 \left\{ \cos^2 \delta \sin^2(\varphi + \frac{\delta}{2}) - \cos^2 \delta \right\} = 16I_{m1}^2 V_m^2 \cos^2 \delta \left\{ \sin^2(\varphi + \frac{\delta}{2}) - 1 \right\} \qquad (8)$$

$$= -16I_{m1}^2 V_m^2 \cos^2 \delta \cdot \cos^2(\varphi + \frac{\delta}{2})$$

Equation (8) is always negative term regardless the values of I_m, V_m, δ and φ. Hence the Cartesian relationship between $(v_1$-$v_2)$ and i_1 represents an ellipse. The approach is shown graphically in Fig. 2 where the instantaneous values of ΔV $(v_1$-$v_2)$ and i_1 are measured at a particular time to calculate the corresponding point on the ΔV- I_1 locus. The graph in Fig. 2 is drawn at a 0.8 lagging power factor.
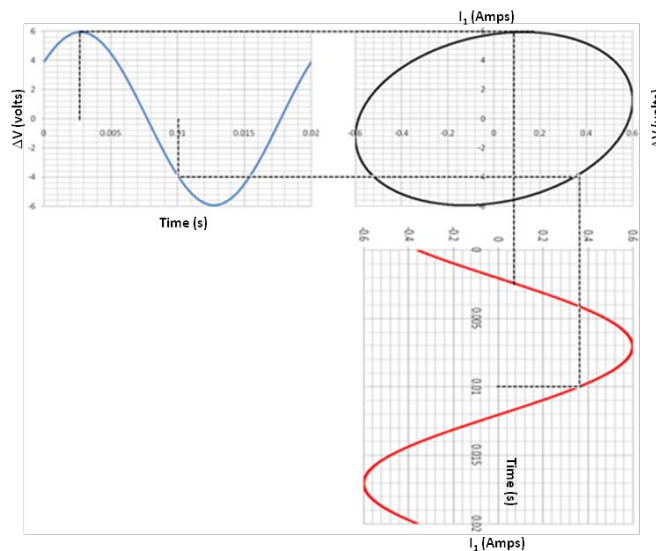

Figure 2
Graphical illustration of the approach

As the phase shift between V_1 and V_2 is normally small, the impact of the angle δ on the locus is insignificant and can be neglected. The phase shift between I_1 and V_2 (φ) is almost equal to the load impedance phase angle as the phase shift between I_1 and I_2 is negligible.

To investigate the impact of the load (Z_L) power factor on the proposed locus, the ΔV-I_1 locus is constructed for a 15-kVA, 2300/230 V single phase transformer with the following equivalent circuit parameters referred to the low voltage side: R_{eq} = 4.45 Ω; X_{eq}= 6.45 Ω; X_m=11 kΩ; R_c= 105 kΩ. Three operating conditions (0.8 lagging power factor, unity power factor and 0.8 leading power factor) with constant impedance magnitude are investigated and the corresponding ΔV-I_1 locus for each case is constructed. The three loci are found to be identical as shown in Fig. 3. Hence, the load power factor has no impact on the proposed locus.
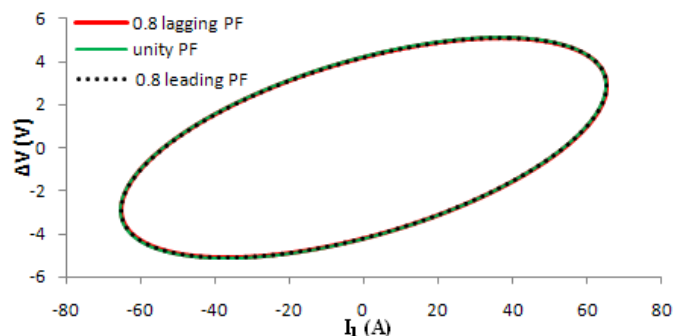

Figure 3
Impact of load PF on the ΔV-I_1 locus

Transformer model

One disk of the distributed transformer model equivalent circuit proposed in this paper is shown in Fig. 4.
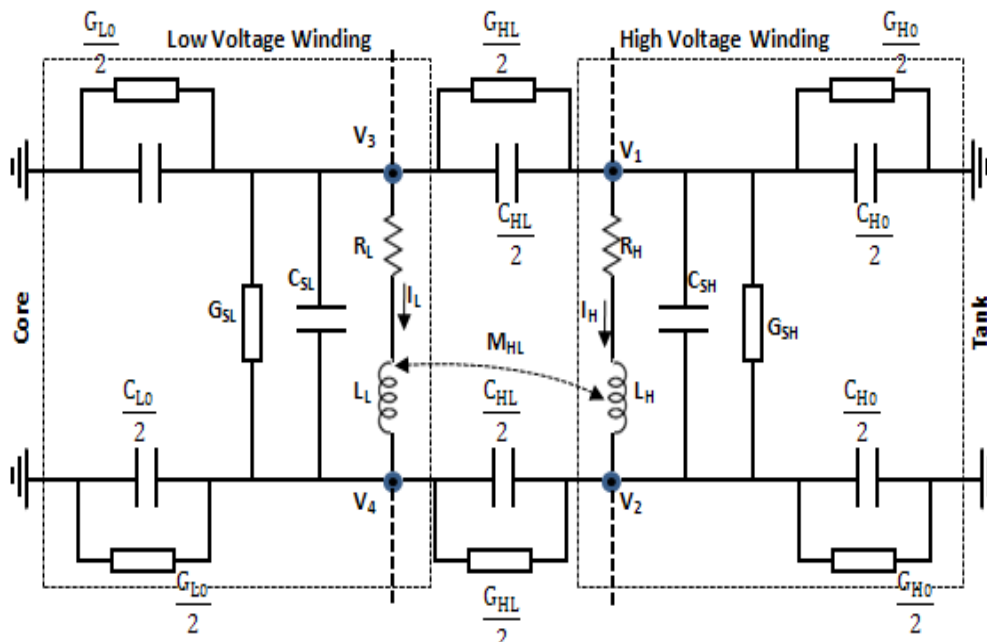

Figure 4
Impact of load PF on the ΔV-I_1 locus

In the model under study, the high voltage (HV) and low voltage (LV) windings are assumed to consist of 100 disks. Each disk comprises series resistance (R) and inductance (L) shunted by a capacitor (C_s) and a conductance (G_s). The capacitance between HV winding and LV winding (C_{HL}) is shunted by dielectric conductance (G_{HL}), also mutual inductances (M_{HL}) between relevant coils are represented. The dielectric insulation between the LV winding and the earthed core and that is between the HV winding and the earthed tank are simulated by a capacitance (C_0) and dielectric conductance (G_0). The physical meaning of the model parameters allows the identification of the problem inside the transformer. Table 1 summaries the transformer model parameters and their influences on particular mechanical faults.

Table 1
Transformer Electrical Parameter and Fault Type Relationship

Physical Parameter	Type of Fault
Inductance	Disk deformation, local breakdown, winding short circuits.
Shunt Capacitance	Disk movements, buckling due to large mechanical forces, moisture ingress, loss of clamping pressure.
Series Capacitance	Ageing of insulation, disk space variation.
Resistance	Shorted or broken disk, partial discharge.

Simulation Results

100 disks (two turns per disk) of the model shown in Fig. 4 is simulated using PSIM software. The model is energized by ac, 50 Hz voltage source of low amplitude and the instantaneous values of v_1, v_2 and i_1 are recorded at a time step of 10 μs. In this way a ΔV-I_1 locus of a healthy transformer can be constructed and is considered as a fingerprint of this transformer. When a transformer experiences an event that results in deformation of the windings, the transformer impedance will vary and this alters the transformer ΔV-I_1 locus diagram.

To investigate the impact of the transformer loading variation on the proposed locus, different load levels at constant power factor are simulated. As can be shown in Fig. 5, increasing the load level from 10 Ω to 20 Ω (100% increment) will not have any impact on the proposed locus.
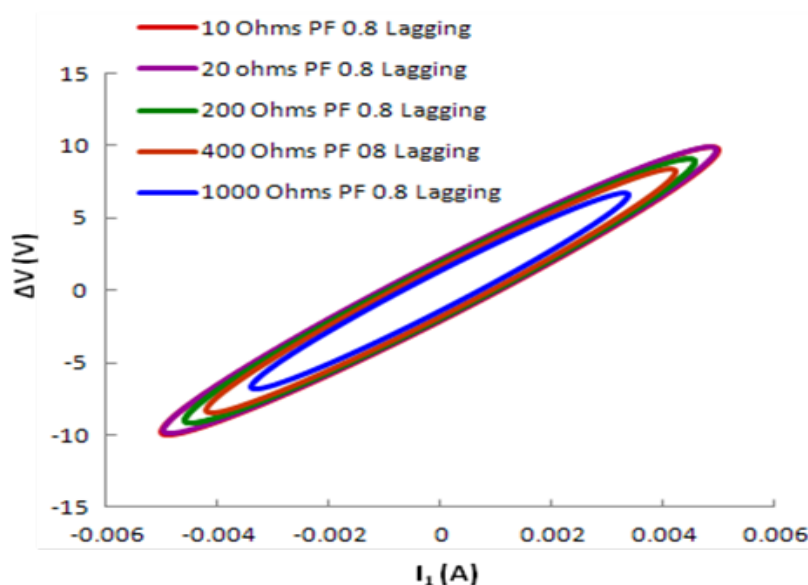

Figure 5
Impact of load magnitude on the proposed locus

The effect of load magnitude on the proposed locus will take place when there is a significant change in load level as evidenced in Fig. 5 when the load magnitude is increased to $200\,\Omega$ as the entire locus area is reduced at this level. However, in all studied cases all loci have the same common major axis and same centroid.

Fault Analysis

Different mechanical faults are simulated on the model and the corresponding ΔV-I_1 loci are plotted and compared with the healthy locus. Diagnosis of the problem is achieved by comparing the healthy transformer fingerprint and the faulty one to identify any differences and hence to determine the possible fault type. In this context, a Matlab code is developed to measure some unique features of the ΔV-I_1 locus such as the semi-major and semi-minor axes lengths and the angle between the major axis and the horizontal axis.

Inter-disk fault

Inter-disk fault is considered as the most common fault of power transformers. Studies show that about 80% of transformer breakdowns are attributed to inter-disk fault [8, 9]. In the model under study, different number of disks has been short circuited to find its impact on the ΔV-I_1 locus. Fig. 6 shows the locus for 30% and 60% faulty disks compared to the healthy locus. It can be observed from the figure that as the number of faulty disks increase, the locus rotates in clockwise direction and its entire area increases.
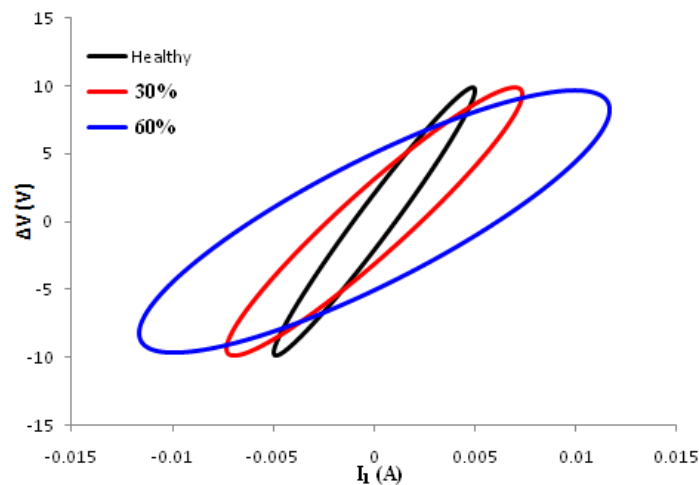

Figure 6
Effect of inter-disk fault on ΔV-I_1 locus

Axial Displacement

This fault occurs due to the magnetic imbalance between the low and high voltage windings due to short circuit currents. The axial displacement between the magnetic centers of the windings results in unbalanced magnetic force components in each half of the winding which leads to a change in its relative position. Leaving this fault unattended can cause winding collapse or failure of the end-supporting structure due to its progressive nature. This type of fault can be simulated by changing the mutual and self inductances of particular disks while change in capacitance can be neglected [10]. In the model under study, axial displacement is modeled by 10% decrease in the inductance. Fig. 7 shows the effect of 30% and 60% axial displacement in the HV winding on the ΔV-I_1 locus. The figure shows that axial displacement decreases the entire area of the locus when compared with the healthy one. Increasing the fault level will further decrease the locus area with no rotation in the locus major axis.
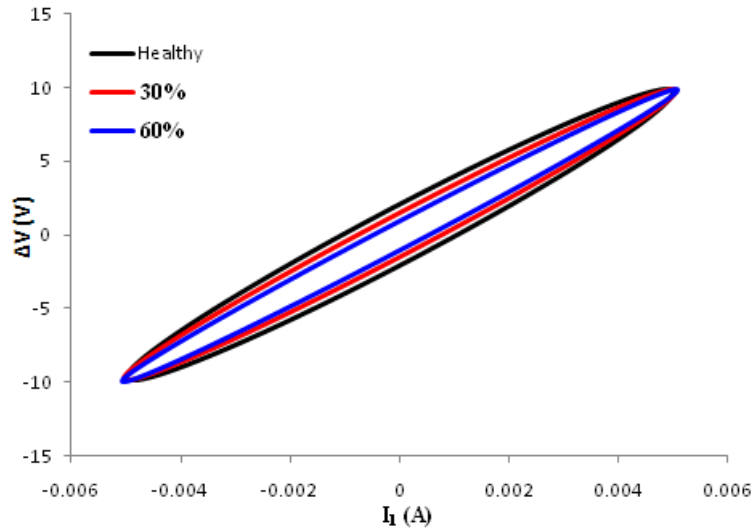
Figure 7
Effect of Axial displacement on ΔV-I_1 locus

Buckling Stress

Leakage flux and current in causes radial force on windings that pulls the inner windings close to the core (buckling stress), while pushing the outer winding toward the limb (tensile stress) [11]. Buckling stress can be simulated in the distributed model by reducing the inter-winding capacitance and the mutual inductance between the windings at the position of deformation. Furthermore, the shunt capacitance is increased due to the reduction of the distance between winding and the core [12]. In this paper, forced buckling is modeled by increasing the shunt capacitance by 10%, decreasing the inductance and series capacitance by 10%. The effect of such fault on the proposed locus is shown in Fig. 8. Unlike axial displacement effect, buckling stress is increasing the locus area and the major axis slightly rotates in the clockwise direction as the number of fault level increases. The slight rotation of the locus major axis discriminates this type of fault from the inter-disk fault.
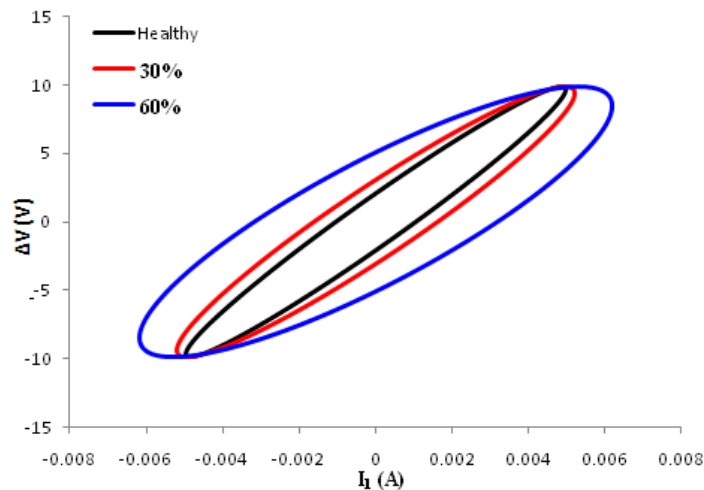

Figure 8
Effect of forced buckling on ΔV-I_1 locus

Leakage (disk to ground) fault

Insulation damage, ground shield damage, abrasion, high moisture content in the winding, hotspot and aging of insulation are the main causes for leakage fault inside a transformer [13]. This type of

fault can be simulated by increasing the shunt conductance and shunt admittance [2]. Fig. 9 shows the effect of increasing the shunt admittance and shunt conductance by 70% on the proposed locus. As can be shown in the figure, the locus area is increasing and the major axis is rotating in clockwise direction similar to the case of inter-disk fault. However, the locus area in case of inter-disk fault is larger than the corresponding locus in case of leakage fault for the same number of faulty disks.
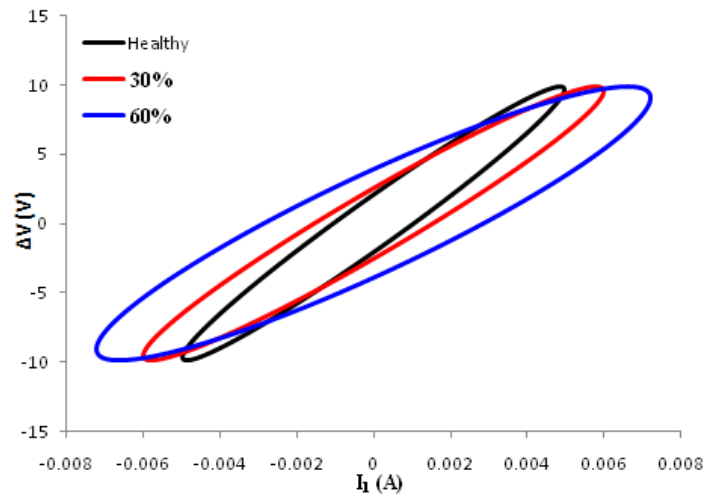

Figure 9
Effect of forced buckling on ΔV-I_1 locus

Disk Space Variation

Mechanical displacements of power transformer windings can be occurred due to short circuit currents. Disk space variation is one of the frequently occurring mechanical faults in power transformer where the geometry of transformer windings is altered. For such fault, the effect of inductance can be neglected with respect to series capacitance at the location of fault [14]. Due to the fact that at low frequency range the transformer winding response is dominated by inductance and the effect of series capacitor is almost negligible, unless there is a significant disk space variation, this type of fault cannot be detected using this technique. In the model under study, this fault is simulated by increasing the series capacitor by 70%. The effect of such fault on the proposed locus is shown in Fig. 10. By increasing the number of faulty disks, the locus is rotating in the clockwise direction and the length of major axis is significantly increasing.
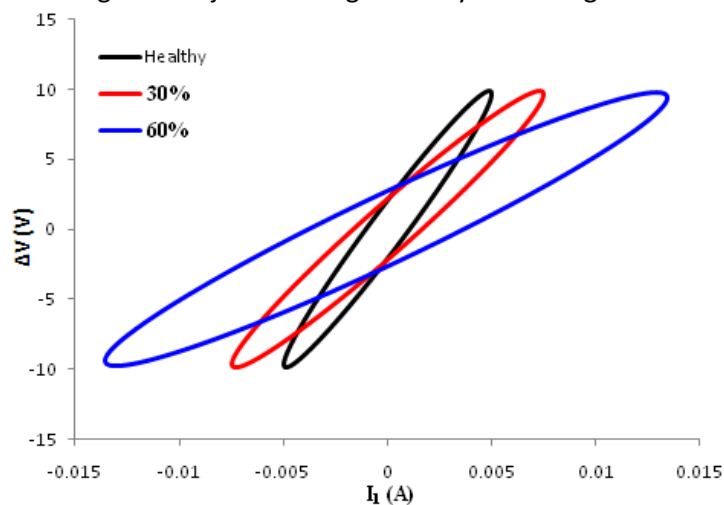

Figure 10
Effect of disk space variation on ΔV-I_1 locus

Visual discrimination

Discrimination between different types of faults can be visibly observed from the $\Delta V - I_1$ locus area and major axis rotation. To show this, different types of faults discussed above are simulated on 80% of the overall disks of the transformer model and the $\Delta V - I_1$ loci for all of them with respect to the healthy locus are compared as shown in Fig. 11 which shows that the locus area is increasing in all faulty cases with respect to the area of the healthy locus except in case of axial displacement where the locus entire area is decreased and the locus major axis is aligning with the healthy major axis. Inter-disk fault has a significant increase in the locus area and its major axis rotates significantly in the clockwise direction. Locus area is increasing in case of forced buckling and leakage fault and both loci are rotating in the clockwise direction with respect to the healthy locus. However, the angle of rotation in case of leakage fault is slightly higher. The disk displacement major axis length is significantly increasing and rotating in the clockwise direction.
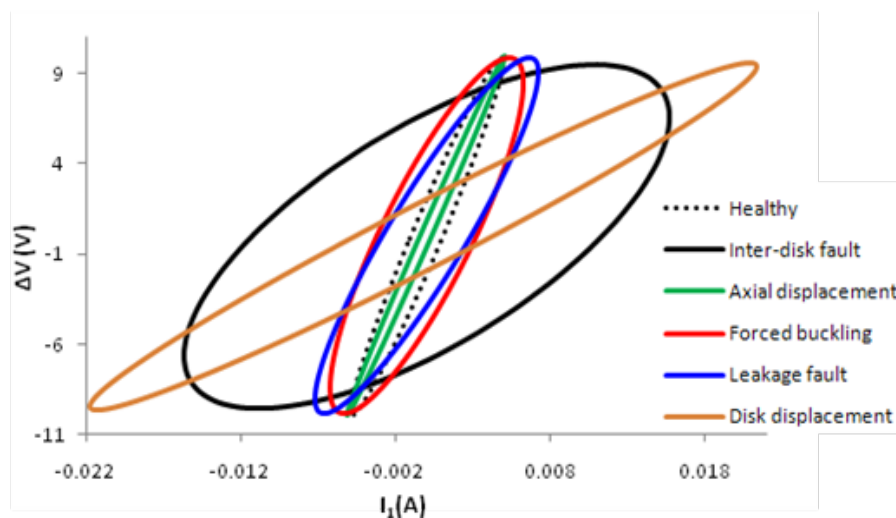

Figure 11
Comparison of the effect of each fault on $\Delta V\text{-}I_1$ locus

Table II summaries the effect of studied faults on the locus area and locus major axis rotation in relative to the healthy locus for visual discrimination.

Table 2
Effect of Faults on Locus Area and Major-Axis Rotation

Fault Type	Area	Rotation
Inter disk	Significant increase	Large
disk space variation	Increase	Very large
Leakage Fault	Increase	Large
Forced buckling	Increase	Slight
Axial displacement	Decrease	None

To show the accuracy of the proposed technique to detect faults simulated in small number of disks, all types of faults are simulated in 5% of the overall disks and the corresponding $\Delta V\text{-} I_1$ loci are plotted as shown in Fig. 12. Same trend can be observed in the impact of each fault on the locus as discussed above. However, it is difficult to visually discriminate different types of faults in this case. A software model is developed to automate the discrimination process and to identify the fault type based on some features of the ellipse as will be discussed in the next section.
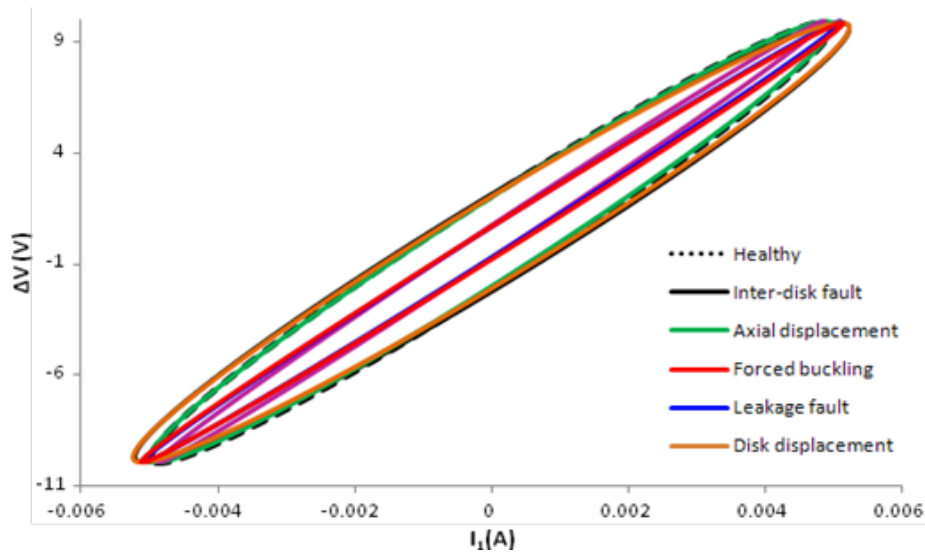
Figure 12
Comparison of the effect of 5% fault level on ΔV-I_1 locus

Discrimination using ellipse features

As has been shown in the mathematical proof and simulation results above, the ΔV-I_1 locus is always representing an ellipse. Some unique features of ellipse can be used to compare different loci in order to identify the type of fault within the power transformer. These features include ellipse centroid, the major and minor axes lengths (a and b respectively), the angle between the major axis and the horizontal axis (θ). A Matlab code is developed to measure these parameters and to calculate the ellipse eccentricity which is used to describe the ellipse general proportion and is given by [7]:

$$e = \sqrt{1 - (\frac{b}{a})^2}$$ (9)

Table 3
Effect of Different Faults on Locus Eccentricity and Axis Rotation

faulty disks	T-T SC fault		Axial displacement		Forced buckling		Leakage fault		Disk space variation	
	e	θ	e	θ	e	θ	e	θ	e	θ
5	0.05	2.15	0.17	0	0.60	1.01	0.60	1.05	0.02	2.23
10	0.24	7.26	0.20	0	0.64	1.56	0.63	1.16	0.02	8.26
15	0.37	8.12	0.21	0	0.65	1.71	0.65	1.60	0.03	9.38
20	0.42	9.59	0.28	0	0.67	1.82	0.73	1.71	0.04	9.71
25	0.47	10.05	0.29	0	0.68	2.01	0.75	1.76	0.06	10.18
30	0.55	11.15	0.35	0	0.69	2.92	0.79	1.90	0.08	11.71
35	1.05	12.28	0.38	0	0.7	3.19	0.81	2.14	0.09	12.60
40	1.11	13.40	0.40	0	0.71	4.69	0.85	2.52	0.12	13.53
45	1.31	13.75	0.42	0	0.73	4.97	0.88	2.74	0.16	14.25
50	1.69	14.21	0.46	0	0.73	5.69	0.97	2.95	0.18	14.81
55	3.13	14.24	0.47	0	0.75	6.15	1.03	3.11	0.19	15.94
60	3.43	15.43	0.52	0	0.81	6.43	1.12	3.56	0.21	16.36
65	4.00	15.84	0.56	0	0.83	7.27	1.33	3.58	0.23	16.48
70	4.21	16.50	0.57	0	0.85	7.97	1.37	3.72	0.25	17.18
75	4.54	16.71	0.58	0	0.87	8.47	1.68	3.98	0.26	17.82
80	4.6	17.05	0.59	0	0.89	8.82	1.68	4.54	0.27	18.09
85	5.2	18.85	0.61	0	0.91	9.22	1.80	4.74	0.29	19.13
90	5.6	19.86	0.63	0	0.66	9.53	1.90	4.87	0.32	19.95
95	5.7	20.89	0.63	0	0.64	10.33	2.01	5.07	0.38	20.93
100	6.61	21.10	0.65	0	0.66	11.05	2.20	5.14	0.49	21.55

To identify the type of fault based on eccentricity and angle of rotation, each fault has been simulated on different number of disks starting from 5 disks to 100 disks and these parameters are calculated for each fault using the developed software as shown in table 3 whish shows the percentage difference in eccentricity (e) and the angle of rotation of the major axis (θ) for different types of faults with respect to the healthy locus. The inter-disk fault significantly increases the eccentricity and angle of rotation as the number of faulty disks increases. Axial displacement does not introduce any effect on the axis rotation and the value of eccentricity is slightly increasing as the number of faulty disks increase. The eccentricity in forced buckling and leakage faults is slightly increasing with the increase of faulty disks however; the increment is more noticeable in case of leakage fault. On the other hand, the increase in the angle of rotation is more significant in case of forced buckling with the increase of faulty disks than the leakage fault especially for large number of faulty disks. The disk space variation has a minor impact on the eccentricity and a significant impact on the angle when the number of faulty disks is increased. Based on the range of the percentage differences of these parameters, the Matlab code is extended to identify the type of fault within the transformer. Five case studies are used to validate the developed approach as below.

Case 1: two identical loci are compared using the developed software which converts the colour of the two loci into white with black background to perform the calculations of ellipse centroide, major and minor axes lengths, eccentricity and the angle between the major axis and the horizontal axis. The software produces the two loci shown in Fig. 13 and shows that there is no difference in eccentricity and angle of rotation of the two loci and hence the software recommends a healthy transformer for this case.
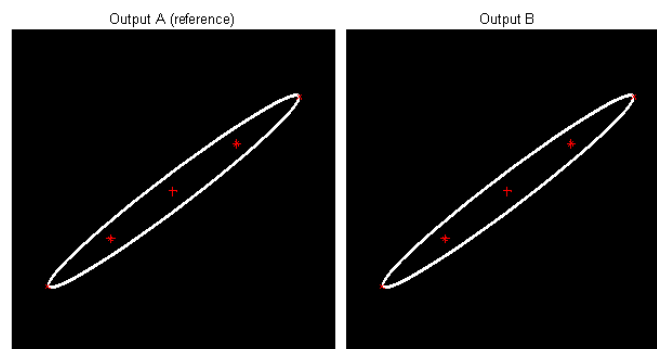

Figure 13
Comparison of two identical loci

Case 2: A forced buckling stress is simulated in 44 disks and the faulty locus is compared with the healthy one using the developed software (Fig. 14). The software gives a 0.72% difference in eccentricity and 4.95% difference in the angle and recommends a forced buckling fault.
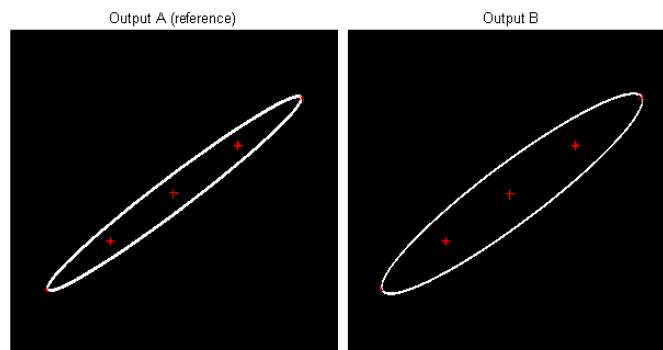

Figure 14
Comparison of faulty and healthy loci

Case 3: An axial displacement fault simulated in 6 disks and the faulty and healthy loci shown in Fig. 15 are compared using the developed software. The software gives a 0.19 % difference in eccentricity and 0 % difference in the angle and recommends an axial displacement fault.
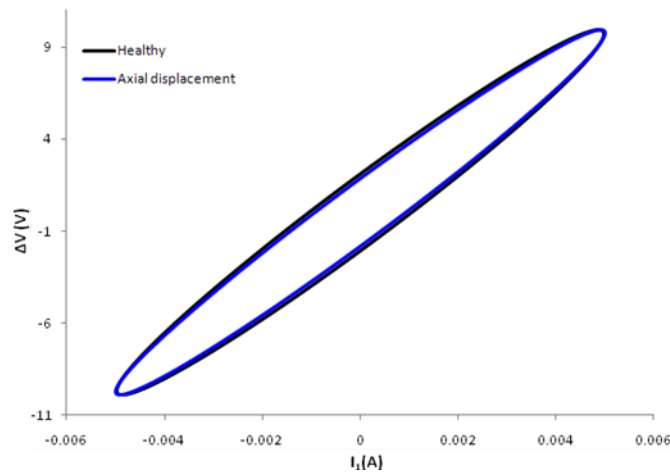

Figure 15
Comparison of a 6-disk axial displacement fault and healthy loci

Case 4: A leakage fault is simulated in 3 disks and the faulty and healthy loci shown in Fig. 16 are compared using the developed software. The software gives a 0.40% difference in eccentricity and a 0.61% difference in the angle and recommends a forced buckling fault.
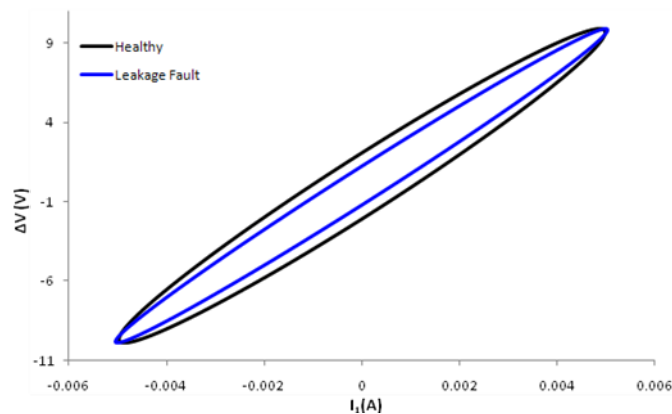

Figure 16
Comparison of a 3-disk leakage fault and healthy loci

Case 5: A disk space variation simulated in 1 disk and the faulty and healthy loci shown in Fig. 17 are compared using the developed software. The software gives a 0.005% difference in eccentricity and 1.6% difference in the angle and recommends a disk space variation.

Case 6: A laboratory experimental testing was performed on a 0.5 kVA, 150/170 V single phase transformer. The transformer is loaded by a 54Ω resistor and a turn -turn short circuit is created on 6% and 15% of the low voltage winding. The ΔV-I_1 locus of the transformer is constructed using a digital oscilloscope. The healthy and faulty loci are compared as shown in Fig. 18 that shows a significant change in the locus area as the number of faulty turns increases. The healthy and 6% short circuit turns loci were fed to the developed software, the percentage difference in eccentricity calculated by the software is 0.21% and the percentage difference in the angle of rotation calculated by the software is 11.9%; these differences are clearly visible in the two loci shown in Fig. 19 that are

generated by the developed software. The significant difference in the angle of rotation aligns well with the range of turn to turn short circuit case shown in table 3.
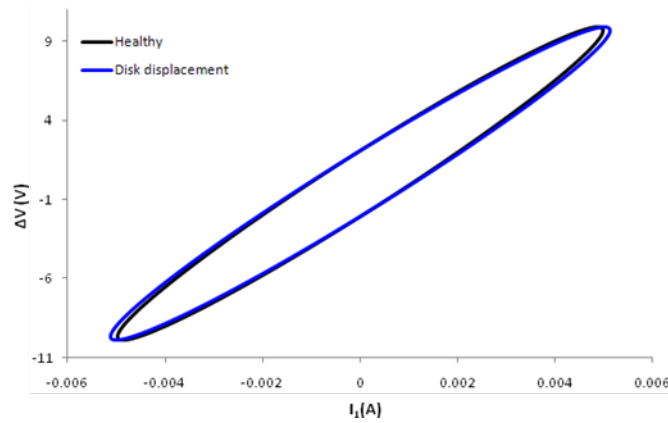

Figure 17
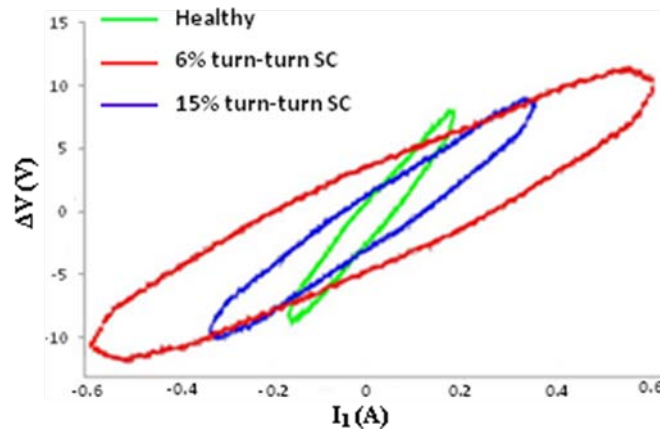Comparison of a 1-disk space variation and healthy loci

Figure 18
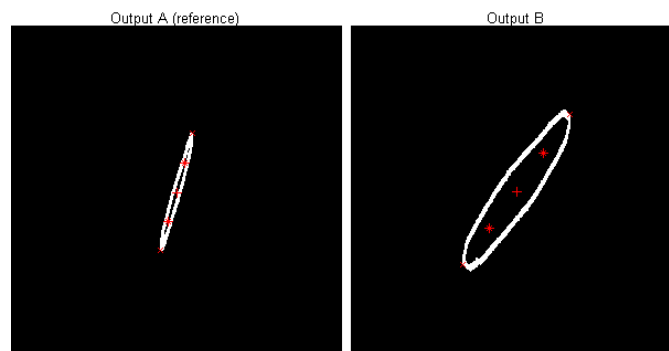Effect of practical Turn to Turn Faults on ΔV-I_1 Locus

Figure 19
Comparison of practical faulty and healthy loci

Conclusion

This paper presents a new technique to identify mechanical faults within a power transformer. The technique relies on constructing a locus diagram of the input and output voltage difference of a particular transformer winding on the Y-axis and the winding input current on the x-axis. This locus is

considered as the finger print of the transformer. Any mechanical fault will alter this locus in a unique way and hence fault detection as well as a fault type can be identified. Digital image processing technique based on measuring and comparing some features of the loci to identify the possible fault type is developed. These features include image centroid, the major and minor axes lengths, eccentricity and the angle of rotation. Simulation results show that each fault has a unique impact on these parameters. The disk space variation has the lowest impact on eccentricity and largest impact on the angle of rotation. The axial displacement does not have any impact on the angle of rotation and has a minor impact on eccentricity. Inter-disk fault has significant impact on angle of rotation and eccentricity while leakage fault has moderate impact on both parameters. Forced buckling has moderate impact on the angle while its impact on the eccentricity is minor. The technique does not call for any new hardware as it uses the existing metering devices attached with the power transformer and can be implemented online as it is performed at the power frequency. The proposed locus can be plotted every cycle (20 ms based on 50 Hz network) and compared with the previous locus using the developed image processing code to immediately identify any changes and generates early warning signal.

References

1. E. J. Figueroa, "Managing an Aging Fleet of Transformers," in *6th Southern africa Regional conference, Cigre 2009*, 2009.

2. S. M. Islam and G. Ledwich, "Locating transformer faults through sensitivity analysis of high frequency modeling using transfer function approach," in *Electrical Insulation, 1996., Conference Record of the 1996 IEEE International Symposium on*, 1996, pp. 38-41 vol.1.

3. M. S. A. Minhas, J. P. Reynders, and P. J. De Klerk, "Failures in power system transformers and appropriate monitoring techniques," in *High Voltage Engineering, 1999. Eleventh International Symposium on (Conf. Publ. No. 467)*, 1999, pp. 94-97 vol.1.

4. A. A. Reykherdt and V. Davydov, "Case studies of factors influencing frequency response analysis measurements and power transformer diagnostics," *Electrical Insulation Magazine, IEEE,* vol. 27, pp. 22-30.

5. H. Firoozi, M. Kharezi, H. Rahimpour, and M. Shams, "Transformer Fault Diagnosis Using Frequency Response Analysis - Practical Studies," in *Power and Energy Engineering Conference (APPEEC), 2011 Asia-Pacific*, pp. 1-4.

6. "Mechanical-Condition Assessment of Transformer Windings Using Frequency Response Analysis (FRA)," CIGRE Working Group A2.26

 2007.

7. G. B. Thomas and R. L. Finney, *Calculus and Analytic Geometry*, 9 ed.: Addison-Wesley, 1996.

8. D. Sharafi, "Life Extension of a Group of Western Power Transformers," in *Power and Energy Engineering Conference (APPEEC), 2010 Asia-Pacific*, pp. 1-4.

9. S. M. Islam, "Detection of shorted turns and winding movements in large power transformers using frequency response analysis," in *Power Engineering Society Winter Meeting, 2000. IEEE*, 2000, pp. 2233-2238 vol.3.

10. E. Rahimpour, J. Christian, K. Feser, and H. Mohseni, "Transfer Function Method to Diagnose Axial Displacement and Radial Deformation of Transformer Winding," *Power Engineering Review, IEEE,* vol. 22, pp. 70-70, 2002.

11. E. Billig, "Mechanical stresses in transformer windings," *Electrical Engineers - Part II: Power Engineering, Journal of the Institution of,* vol. 93, pp. 227-243, 1946.

12. J. A. S. B. Jayasinghe, Z. D. Wang, P. N. Jarman, and A. W. Darwin, "Winding movement in power transformers: a comparison of FRA measurement connection methods," *Dielectrics and Electrical Insulation, IEEE Transactions on,* vol. 13, pp. 1342-1349, 2006.

13. G. Junfeng, G. Wensheng, T. Kexiong, and G. Shengyou, "Deformation analysis of transformer winding by structure parameter," in *Properties and Applications of Dielectric Materials, 2003. Proceedings of the 7th International Conference on*, 2003, pp. 487-490 vol.1.

14. E. rahimpour and S. Tenbohlen, "Experimental and Theoretical Investigation of Disc Space Variation in Real High-Voltage Windings using Transfer Function Method," *IET Electrical Power Application,* vol. 4, pp. 451-461, 2010.

Ahmed Abu-Siada is a senior lecturer at Curtin University, Western Australia. He earned B.Sc. and M.Sc. degrees from Ain Shams University, Cairo and the PhD degree from Curtin University, Western Australia, all in Electrical Engineering. His research interests include power system stability, Condition monitoring, Power Electronics, Power Quality, Energy Technology and System Simulation.